Propagation of the Superthermal Corona from CO_2-Laser-Irradiated Microtargets

R. S. Marjoribanks, M. D. J. Burgess, G. D. Enright, and M. C. Richardson
Division of Physics, National Research Council of Canada, Ottawa K1A 0R6, Canada
(Received 23 July 1980)

The propagation of the superthermal plasma from microdisk targets irradiated with single, nanosecond CO_2 laser pulses at intensities of $\sim 10^{14}$ W cm^{-2} is examined through the study of its effect on subsidiary passive targets. The observed propagation velocity is similar to the estimated superthermal ion acoustic speed and has an intensity dependence of $I^{0.14-0.21}$.

PACS numbers: 52.50.Jm, 52.25.Fi, 52.40.Hf, 52.40.Kh

It is now generally accepted that the interaction of intense nanosecond CO_2 laser radiation with solid targets is dominated by collisionless processes which couple energy into fast electrons.[1-4] The generation of these hot electrons is of considerable concern to current laser-fusion studies since (i) they can penetrate into the target interior prior to peak compression, causing serious preheat, and (ii) they can establish an ambipolar field about the target and thus lose their energy to directed ion motion. A particular consequence can be effective decoupling of energy from the high-density thermal corona, a general concern first pointed out by Kidder and Zink.[5] This Letter addresses the second of these issues, the propagation of the superthermal corona comprised of fast ions having motion directed outward from the target[6] and fast electrons which, being confined by the time-dependent coronal fields,[7] make many transits of the coronal plasma.[8] Reflection of these electrons can result in energy loss to the coronal fields,[7] implying a higher initial electron energy than is directly deduced from either x-ray continuum emission[9] or fast-ion spectra.[10]

The present investigations examined the propagation of the superthermal corona by observing its effect on subsidiary disk targets mounted some distance behind the irradiated target, as in Fig. 1(a). The front disk target, Al or $(CH_2)_n$, with a thickness in the range 10–100 μm and a diameter of 500 μm–1 mm, was irradiated by a single pulse from the COCO-II laser system of ~1.4 ns duration (full width at half maximum) and intensity of $\sim 10^{14}$ W cm^{-2} in a focal spot with a half-energy diameter of ~100 μm.

Evidence has already been presented for anomalous lateral energy transport on similar single-disk targets.[11] These studies showed that a significant fraction of absorbed laser energy is coupled to the rear surface of the target. In particular, the asymptotic distribution of plasma energy was seen[11,12] to be strongly peaked in the forward and rearward directions. For a typical disk-pair target used in the present experiments, this distribution indicates that the secondary target might be expected to intercept ~5% of the laser energy originally absorbed at the front target. This type of energy transfer is evident in Fig. 1(b) which shows an x-ray (>0.6 keV) pinhole photograph of a 500-μm-diam, 150-μm-thick Al disk-pair target. As was previously noted,[11] strong x-ray emission is observed from the rear of the irradiated target, implying the formation of a high-temperature

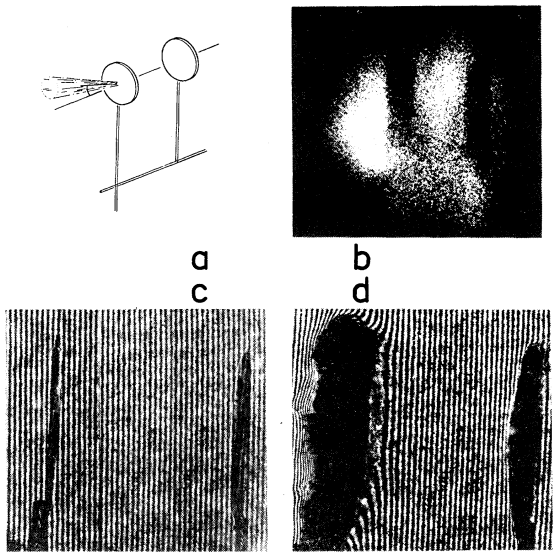

FIG. 1. (a) Schematic representation of target configuration with second disk situated 300 μm–3 mm behind irradiated target disk. (b) X-ray pinhole photograph of irradiated disk pair, including size and separation. Energy ~20 J incident onto left target, from left. Interferometry: (c) Disk pair, 12.5-μm-thick Al disks, 500 μm diameter, 500 μm separation. Before irradiation. (d) Same disk pair as in (c), irradiated by 8.6 J COCO-II laser pulse, 1.3 ns after the 20% intensity point in pulse leading edge.

plasma. However, as can be seen in Fig. 1(b), a separate, distinct plasma having comparable x-ray emission is also created on the front surface of the passive target, situated ~400 μm behind the irradiated target.

The plasma formed on these targets was also investigated at various times during the interaction by picosecond interferometry, using a folded-wave-front interferometer illuminated by a synchronized 0.53-μm, 50–150-ps probe pulse.[13] Figures 1(c) and 1(d) show a disk-pair target (12 μm thickness, 500 μm diameter, and 500 μm separation) before and near the end of a 9-J irradiating pulse. It can be seen that during irradiation, an appreciable plasma has developed uniformly over the front of the second target, whereas the thermal plasma on the rear of the front disk has not expanded beyond ~150 μm. The expansion velocity of the isodensity surface at 10^{19} cm^{-3} from the passive target is $\sim 5\times10^{6}$ cm s^{-1} and, assuming an isothermal blowoff, the electron temperature T_e is estimated to be 20 eV. The flat, constant gradient density profile deduced from the interferogram is consistent with a thermal plasma formed by a uniform bath of energy from the superthermal corona.

Resolution of the temporal development of plasma on the secondary target relative to that on the irradiated target was provided by streak photography using an S-1 photocathode, picosecond streak camera. By spatially imaging the disk pairs with their common normal axis along the streak slit, plasma onset and expansion of the visible (~750–1100 nm) emission zones were recorded. Streak photographs such as Fig. 2(a) illustrate the creation of plasma on the passive target long before the region of visible emission from the rear side of the irradiated target reaches it. The velocity of expansion measured for either plasma is $(6-8)\times10^{6}$ cm s^{-1}, of the same order as that of the irradiated plasma. Along with interferograms and x-ray pinhole photographs, this implies that plasma temperatures on the passive target and on the rear side of the irradiated target are comparable.

By varying the target disk-pair separation at a particular irradiance (~10^{14} W cm^{-2}) it was found that the relative delay of onset of visible emission from the passive target, Fig. 2(b), could be related to a propagation velocity of $(1.0\pm0.1)\times10^{8}$ cm s^{-1} (allowing for the total path length to be the distance from the focal spot to target edge plus the separation distance). It is interesting to note that this velocity, characterizing the expansion in a vacuum, is similar to those recently estimated[14–16] in relation to the propagation of energy along surfaces.

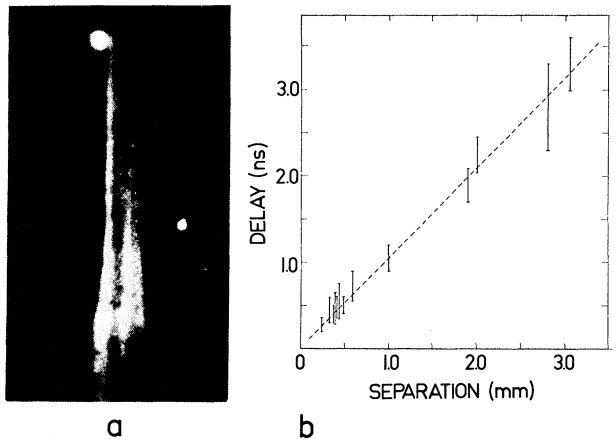

FIG. 2. (a) Streak photograph of luminous regions of disk-pair target; each disk 500 μm diameter, 150 μm thick; separation 300 μm. (b) Delay of onset of luminosity from front of second (passive) target as a function of target separation, relative to first target. $I\sim10^{14}$ W cm^{-2}. Deduced velocity of $(1.0\pm0.1)\times10^{8}$ cm s^{-1} allows inclusion of half-diameter of irradiated disk in path length.

It is graphically evident that the formation of plasma on the second disk cannot result from the propagation of the thermal plasma from the irradiated disk. Moreover, in separate experiments in which the glass stalk supports of the microdisk targets (normally 2 mm long) were doubled in length, no change was noted in the delay between onset of the principal and subsidiary plasmas, thus eliminating any disk-to-disk return-current effects[17] in these observations. Coupling of energy to the passive target by direct soft x-ray pumping from the irradiation zone is ruled out as the luminosities and expansion velocities of the observed plasmas were independent of front target thickness, in the range 10–100 μm. It is more difficult to rule out soft x rays emanating from the rear of the irradiated disk as the cause of the plasma on the second target. However, x-ray pinhole photographs which show that the passive target is, in general, a brighter x-ray emitter than the rear surface of the front foil and the comparable temperatures inferred for these plasmas cannot be explained by this mechanism alone.

The times in which an appreciable rate of energy deposition around and between these targets begin suggest that the formation of the plasma on

the rear side of the irradiated target, and on the front surface of the passive target, is governed by the outward propagation of the superthermal corona. It is surmised that initially the irradiated target acquires a high potential due to accelerated hot electrons which leave the interaction zone entirely, or make large amplitude orbits around the target.[11] A plasma sheath formed about the target will expand at roughly the superthermal ion acoustic velocity,[18] $c_H \sim (kT_H Z/m_i)^{1/2}$, where Z/m_i is the mean charge-to-mass ratio of the superthermal ions. A mean value of $Z \sim 12$ for Al targets[10] and a measured value of $T_H \sim 17.5$ keV for a 500-μm-diam target at an irradiance of 10^{14} W cm^{-2} [19] gives a value of $c_H \sim 0.9 \times 10^8$ cm s^{-1}, in reasonable agreement both with these and the earlier observations.[14] The presence of hydrocarbon contaminants in the fast-ion blowoff would yield a value marginally higher.

That the propagation velocity measured in this study is thus consistent with hot electron temperatures of tens of kiloelectronvolts, but inconsistent with thermal plasma temperatures, is reinforcement of the notion that fast electrons are transported within the plasma sheath to the rear side of the irradiated target during the laser pulse. Stronger evidence that the plasma created on the subsidiary target results from its interception of the superthermal corona propagating by this principle is obtained from study of the intensity dependence of the velocity of propagation deduced from the streak photographs, Fig. 3, which shows that $c_H \propto I^{0.14-0.21}$. This is in good agreement with the dependence of $T_H \propto I^{0.25-0.40}$ measured under similar irradiation conditions[9] and with the predictions of simulations.[3-4]

The present experiments provide direct evidence for energy deposition on surfaces remote from the interaction region on a superthermal ion acoustic time scale. The intersection of the leading edge of the superthermal corona and the target surface delimits the lateral energy transport as a result of the interception of the laser-produced fast electrons by the target.[14,16] Targets with dimension $d \ll c_H \tau_L$ (where τ_L is the laser pulse length) would be enveloped by the superthermal corona and the absorbed energy may then be effectively decoupled from the thermal plasma. The implication for inertial fusion schemes with intense CO_2 laser is that the target diameter must be greater than $c_H \tau_L$ to ensure that the absorbed laser energy, which initially resides in fast electrons, can be efficiently coupled into the imploding target.

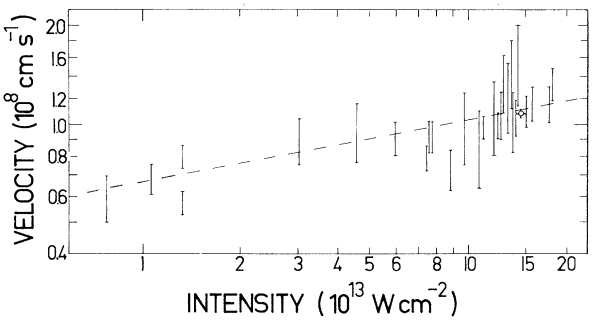

FIG. 3. Variation of the velocity of propagation of the superthermal corona with intensity; $c_H \propto I^{0.14-0.21}$. Dashed line corresponds to $I^{0.18}$; circle corresponds to velocity found in Fig. 2(b).

The authors wish to thank P. A. Jaanimagi for his invaluable assistance in setting up the picosecond streak camera and to acknowledge valuable discussions with him and D. M. Villeneuve. We also wish to thank Y. P. Lupien for the fabrication of the disk-pair targets, and G. A. Berry, P. Burtyn, and R. W. Sancton for their continuing technical assistance. The work by one of us (R.S.M.) was performed in partial fulfillment of the M. Sc. degree, University of Toronto, Toronto, Canada.

[1]D. W. Forslund, J. M. Kindel, K. Lee, E. L. Lindman, and R. L. Morse, Phys. Rev. A 11, 679 (1975).
[2]K. G. Estabrook, E. J. Valeo, and W. L. Kruer, Phys. Fluids 18, 1151 (1975).
[3]D. W. Forslund, J. M. Kindel, and K. Lee, Phys. Rev. Lett. 39, 284 (1977).
[4]K. G. Estabrook and W. L. Kruer, Phys. Rev. Lett. 40, 42 (1979).
[5]R. E. Kidder and J. W. Zink, Nucl. Fusion 12, 235 (1972).
[6]E. J. Valeo and I. B. Bernstein, Phys. Fluids 19, 1348 (1976).
[7]K. A. Brueckner and Y. M. Lee, Nucl. Fusion 19, 1431 (1979).
[8]J. R. Albritton, I. B. Bernstein, E. J. Valeo, and E. A. Williams, Phys. Rev. Lett. 39, 1536 (1977).
[9]G. D. Enright, M. C. Richardson, and N. H. Burnett, J. Appl. Phys. 50, 3909 (1979).
[10]C. Joshi, M. C. Richardson, and G. D. Enright, Appl. Phys. Lett. 34, 625 (1979).
[11]N. A. Ebrahim, C. Joshi, D. M. Villeneuve, N. H. Burnett, and M. C. Richardson, Phys. Rev. Lett. 43, 1995 (1979).
[12]D. M. Villeneuve *et al.*, to be published.
[13]R. Fedosejevs and M. C. Richardson, to be published.

[14]R. S. Marjoribanks, M. D. J. Burgess, C. Joshi, G. D. Enright, and M. C. Richardson, Bull. Am. Phys. Soc. 24, 1027 (1979).
[15]A. W. Ehler, F. Begay, T. H. Tan, and P. H. Castine, J. Phys. D 13, L65 (1980).
[16]R. Fedosejevs, M. D. J. Burgess, G. D. Enright, and M. C. Richardson, to be published.
[17]R. F. Benjamin, G. H. McCall, and A. W. Ehler, Phys. Rev. Lett. 42, 890 (1979).
[18]The discussion presented here is similar to that which has been used to explain how vacuum insulation would reduce direct fast-electron preheat of the fuel for laser-fusion targets. See for example, K. Lee, D. W. Forslund, J. M. Kindel, and E. L. Lindman, Nucl. Fusion 19, 1447 (1979).
[19]M. C. Richardson, M. D. J. Burgess, N. H. Burnett, N. A. Ebrahim, G. D. Enright, R. Fedosejevs, P. A. Jaanimagi, C. Joshi, R. S. Marjoribanks, and D. M. Villeneuve, in Proceedings of the Fifth Workshop on Laser Interaction and Related Plasmas, Rochester, edited by Helmut J. Schwarz and Heinrich Hora (to be published).

Study of Ablatively Imploded Spherical Shells

M. H. Key, P. T. Rumsby, and R. G. Evans
Rutherford Laboratory, Chilton, Didcot, Oxfordshire, United Kingdom

and

C. L. S. Lewis, J. M. Ward, and R. L. Cooke
Queen's University, Belfast, United Kingdom

(Received 30 July 1980)

The implosion of spherical-shell targets driven ablatively by six 1.05-μm laser beams at an irradiance of $\sim 10^{13}$ W cm^{-2} has been studied by streak time-resolved x-ray shadowgraphy. Measurements of acceleration determined the ablation pressure. Departures from one-dimensional simulations showed increasingly degraded implosions as the shell aspect ratio $r/\Delta r$ was increased from 10 to 110 for shells with surface perturbations of $\pm 0.05\Delta r$.

PACS numbers: 52.50.Jm, 47.20.+m, 52.55.Mg, 52.70.-m

Compression of plasma in laser-driven implosions has been characterized as "ablative" or "exploding pusher" according to the relative importance of surface ablation pressure and bulk pressure due to preheating by electrons. To date, experimental study of ablative implosions has been limited,[1] partly because their high-density low-temperature plasma yields little diagnostic information in the form of x-ray or fusion-product emission compared with exploding-pusher implosions.[2] The development of x-ray probing techniques[3] has alleviated this problem and permitted study of the implosion dynamics of spherical-shell targets under ablative acceleration with use of streak time-resolved x-ray shadowgraphy.[4]

Elementary mechanics show that for negligible mass loss, a spherical shell with ratio of radius to wall thickness (aspect ratio) $r/\Delta r$ and density ρ can be accelerated to a velocity v of the order $(P_a r/\Delta r)^{1/2}$ by a surface ablation pressure P_a. Since the stagnation pressure P_f of the implosion is of the order ρv^2 it follows that $P_f \propto P_a r/\Delta r$. High aspect ratio therefore leads to high stagnation pressure. However, the acceleration of the dense shell by the low-density ablation plasma is subject to the Rayleigh-Taylor instability, whose classical growth exponent for perturbations of wavelength $\lambda \sim \Delta r$ is approximately $(2\pi r/\Delta r)^{1/2}$ during an implosion. Since the instability growth depends on the aspect ratio it is expected to limit the maximum aspect ratio and stagnation pressure. Detailed theoretical work has, however, yielded contradictory results, some finding growth rates close to classical[5] and some predicting stabilizing effects due to factors not considered in the classical Rayleigh-Taylor theory such as thermal conduction and ablation flow through the unstable region.[6] Such contradictions emphasize the value of experimental study of the stability of ablative implosions of shells of increasing aspect ratio as described here.

Our experimental arrangement is illustrated in Fig. 1. Six beams of 1.05-μm laser light irradiate the microballoon target and a seventh is focussed on a horizontal Al-foil x-ray-backlighting target. The microballoon is viewed along a hori-

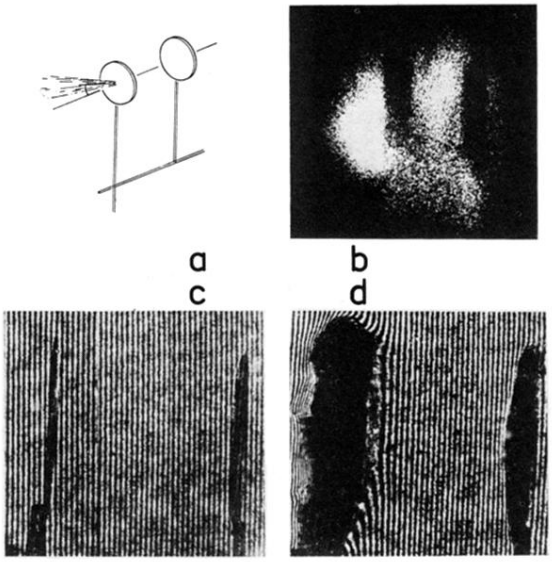

FIG. 1. (a) Schematic representation of target configuration with second disk situated 300 μm–3 mm behind irradiated target disk. (b) X-ray pinhole photograph of irradiated disk pair, including size and separation. Energy ~20 J incident onto left target, from left. Interferometry: (c) Disk pair, 12.5-μm-thick Al disks, 500 μm diameter, 500 μm separation. Before irradiation. (d) Same disk pair as in (c), irradiated by 8.6 J COCO-II laser pulse, 1.3 ns after the 20% intensity point in pulse leading edge.

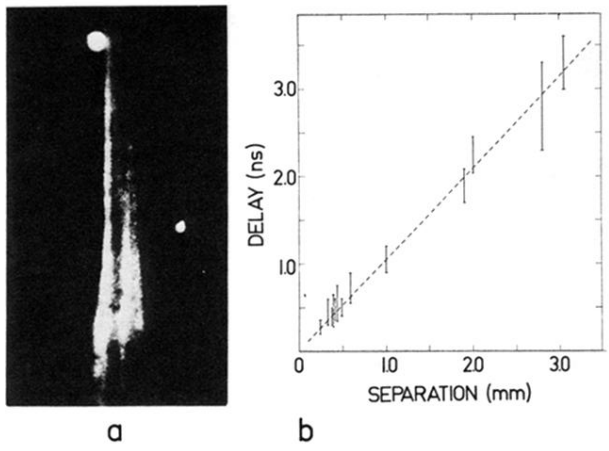

FIG. 2. (a) Streak photograph of luminous regions of disk-pair target; each disk 500 μm diameter, 150 μm thick; separation 300 μm. (b) Delay of onset of luminosity from front of second (passive) target as a function of target separation, relative to first target. $I \sim 10^{14}$ W cm^{-2}. Deduced velocity of $(1.0 \pm 0.1) \times 10^{8}$ cm s^{-1} allows inclusion of half-diameter of irradiated disk in path length.